

Spatiotemporal Pulses in a Liquid Crystal Optical Oscillator

U. Bortolozzo,¹ A. Montina,² F. T. Arecchi,² J. P. Huignard,³ and S. Residori⁴

¹Laboratoire de Physique Statistique de l'ENS, 24 rue Lhomond, 75231 Paris Cedex 5, France

²Physics Department, University of Florence, Largo E. Fermi 6, 50125 Florence, Italy

³Thales Research & Technology, RD 128 91767 Palaiseau Cedex, France

⁴INLN, Université de Nice Sophia Antipolis, CNRS; 1361 route des Lucioles, 06560 Valbonne, France

(Received 29 January 2007; published 11 July 2007)

A nonlinear optical medium results by the collective orientation of liquid crystal molecules tightly coupled to a transparent photoconductive layer. We show that such a medium can give a large gain; thus, if inserted in a ring cavity, it results in an unidirectional optical oscillator. We report new dynamical regimes characterized by the generation of spatiotemporal pulses, localized in three dimensions and arising from the random superposition of many longitudinal and transverse modes with different frequencies.

DOI: 10.1103/PhysRevLett.99.023901

PACS numbers: 42.65.Sf, 05.45.-a, 42.70.Df, 61.30.-v

Optical oscillators have been extensively studied in the past; in particular, ring cavities with photorefractive gain [1,2] have attracted much attention, both experimentally and theoretically [3,4]. Here we present a different optical medium that results from the collective orientation of liquid crystal molecules tightly coupled to a photoconductive layer and pumped in a two-wave mixing configuration [5,6]. We show for the first time that, when inserted in a ring cavity, the liquid crystal light valve has a gain large enough to overcome the losses, thus resulting in a unidirectional optical oscillator. The wide transverse size and the high nonlinearity of the liquid crystal light valve allows us to explore dynamical regimes where a huge number of longitudinal and transverse modes are interacting. Up to date such regimes have remained inaccessible for all the known types of optical cavities.

In particular, we report here the observation of high amplitude spatiotemporal pulses appearing in random space points and confined along the three space directions. Even though several theoretical predictions have been given in the past of 3D confined optical structures [7–9], we give here the first experimental evidence. We present also a theoretical model for the liquid crystal oscillator that takes into account the longitudinal dependence of the field, thus allowing for the formation of 3D structures. For a set of parameters consistent with the experiment, we perform numerical simulations confirming the appearance of 3D localized spatiotemporal pulses. It is worth, here, to distinguish spatiotemporal pulses from the localized structures that arise when a system presents bistability between a spatially homogenous state and a pattern state [10]. Indeed, spatiotemporal pulses originate from a coherent superposition randomly taking place within a large number of coexisting modes and are space-time localized, while localized structures are isolated cells of a corresponding spatial pattern and are confined only in space, living for indefinite time if not erased by a local, and large enough, perturbation. Spatiotemporal pulses are somehow reminiscent of the pulsating solitons predicted in the complex Ginzburg-Landau equation for mode-locked lasers [11]

or of the random-phase solitons found in the nonlinear Schrödinger equation for nonlinear lattices [12]. As in this latter case, we have a large time scale separation between the fast decay of the field in the cavity ($\tau_c \approx 10^{-7}$ s) and the slow response time of the medium ($\tau \approx 10^{-3}$ s for liquid crystals); thus, the dynamics is slaved by the slow evolution of the refractive index. However, in our experiment the randomness of the field is not introduced by external perturbations but it spontaneously arises from the simultaneous presence of a huge number of cavity modes interacting through the nonlinear medium. Note that similar mechanisms are at the basis of the collapsing filaments predicted in optical turbulence [13] and have been recently employed to synthesize spatiotemporal pulses in a linear optical system [14].

The experimental setup is schematically represented in Fig. 1. The cavity, that has a total cavity length $L = 240$ cm, consists of three high-reflectivity dielectric mirrors and a lens of $f = 70$ cm focal length. The coordinate system is taken such that z is along the cavity axis and x, y are on the transverse plane. The cavity lens is positioned at $z = 150$ cm, where $z = 0$ is the entrance plane of the liquid crystal light valve (LCLV). This configuration enhances the mode stability, providing a nearly spherical configuration, and ensures the presence of different longitudinal modes oscillating at different frequencies. The gain medium is a LCLV with one of the walls made of a thin

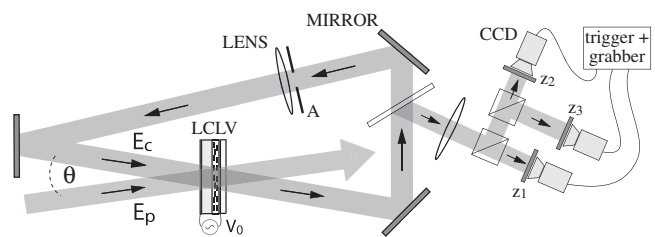


FIG. 1. Experimental setup; A is an aperture fixing the Fresnel number of the cavity, $z = 0$ corresponds to the plane of the LCLV; z_1, z_2, z_3 are the three different observation planes.

slice, 1 mm thickness, of the photoconductive $B_{12}SiO_{20}$ (BSO) crystal [6]. An external voltage V_0 is applied to the LCLV by means of transparent electrodes deposited over the glass window and the external side of the BSO crystal. The BSO acts as a transparent photoconductor, thus modulating the voltage across the liquid crystals as a function of the intensity of the light passing through the cell [5]. The working point of the liquid crystals is fixed at $V_0 \approx 20$ V, frequency 25 Hz. The thickness of the liquid crystal layer is $d = 14 \mu\text{m}$ and the lateral size of the cell is $20 \times 30 \text{ mm}^2$. The cell is pumped by an enlarged and collimated (10 mm diameter) beam from an Ar^+ laser ($\lambda = 514 \text{ nm}$), intensity $I_p \approx 2 \text{ mW/cm}^2$.

The light amplification in the cavity is based on two-wave mixing (2WM) interactions in the liquid crystals [6]. The pump beam and the cavity axis are at an angle $\theta = 30 \text{ mrad}$. The pump polarization is linear and parallel to the liquid crystal director orientation. The cavity field E_c is spontaneously generated; it is polarized along the vertical direction, since only the extraordinary waves are amplified by the 2WM, and it has a frequency almost equal to that of the pump field E_p . In fact, we observe a frequency detuning of a few Hz, which is automatically selected by the cavity in order to maximize the gain and that corresponds to a refractive index grating slowly moving inside the liquid crystals. It is well known that a moving grating enhances the two-wave mixing gain for photorefractive crystals [15]; however, this frequency shift was not observed before for a liquid crystal light valve. Also note that the LCLV is a thin medium, so that the 2WM here takes place in the Raman-Nath regime [16]. The Fresnel number of the cavity, which is the ratio of the area of the diffraction limiting aperture to the area of the fundamental Gaussian mode, is controlled by a diaphragm placed in the cavity and can be changed from $F = 1$ to approximately $F = 500$, which implies changing from a single transverse mode oscillation to a regime where a huge number of modes are interacting. An important feature, that differentiates our system from previous photorefractive cavities, is that changing the voltage V_0 changes the uniform refractive index n_c of the liquid crystals, and thus the frequency detuning between the lowest order cavity mode and the pump beam. In order to compensate the detuning, the cavity adjusts its emission by changing the length of the out of axis transverse wave vectors [17], so that the number of active modes can be changed by keeping the Fresnel number fixed and by varying the voltage V_0 .

For the purpose of visualization, a small fraction (4%) of the cavity field is extracted by a beam sampler and, after passing through a lens, is separated into three distinct optical paths. Three CCD cameras (see Fig. 1) record the transverse intensity distributions at three different planes located at z_1 , z_2 , and z_3 . In the first set of experiments, we use one CCD at $z_1 = 0 \text{ cm}$ and fix the Fresnel number at $F = 500$. By changing V_0 and the pump intensity I_p , we

have determined the experimental phase diagram, as reported in Fig. 2(a). Cavity mode oscillations are in the larger gray area whereas spatiotemporal pulses are in the darker area. The low V_0 regimes are similar to those previously reported for low F photorefractive cavities, with the alternation of low order Gauss-Laguerre modes [1,2]. The transition to the high V_0 regimes is accompanied by the emission of high order and out of axis symmetrical modes. For intermediate values of V_0 and I_p , a large number of modes interact through the nonlinear medium and give rise to the formation of spatiotemporal pulses, appearing as large intensity peaks over a lower amplitude and “specklelike” background. Instantaneous snapshots of the transverse intensity distributions $I_c(x, y)$ are displayed in Fig. 2(b)–2(g). The transverse size of the oscillating field increases with V_0 , up to a large ring for high V_0 . The spatiotemporal pulses appear when a large number of modes is populating the whole size of the area illuminated by the pump beam. A typical snapshot corresponding to this case is displayed in Fig. 2(g) and the corresponding spatiotemporal plot is shown in Fig. 2(h).

To investigate the dynamics of spatiotemporal pulses we have fixed $V_0 = 20.3 \text{ V rms}$ and $I_p = 2.0 \text{ mW/cm}^2$, and we have recorded several movies. The spatiotemporal pulses are identified by applying on each frame a threshold of 3 times the average intensity \bar{I}_c calculated over the entire set of frames in any experimental run. The extension of the pulses in the z direction is investigated by simultaneously recording the intensity distributions at the three planes z_1 , z_2 , and z_3 plane. The three CCD are driven by the same trigger, whose delay time is negligible with respect to the

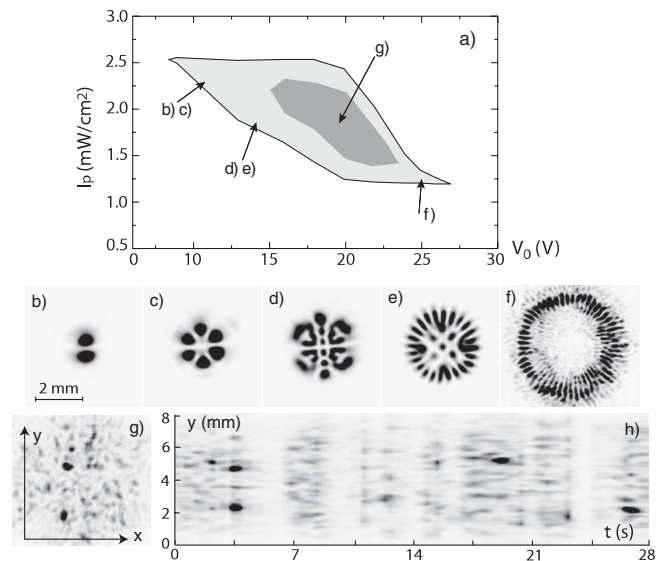


FIG. 2. (a) Experimental phase diagram and instantaneous snapshots taken at (b), (c) $V_0 = 10 \text{ V}$, $I_p = 2.4 \text{ mW/cm}^2$, (d), (e) $V_0 = 14 \text{ V}$, $I_p = 2.0 \text{ mW/cm}^2$, (f) $V_0 = 25 \text{ V}$, $I_p = 1.3 \text{ mW/cm}^2$, (g) $V_0 = 20 \text{ V}$, $I_p = 2.0 \text{ mW/cm}^2$; (h) space-time plot obtained for the same parameter values as in (g).

liquid crystal response time. We select $z_1 = 0$, $z_2 = 5$, and $z_3 = 32$ cm. The magnification ratio, the size of the window, and the intensity levels are the same for the three planes. Three spatial profiles recorded at the three different planes are displayed in Fig. 3. By cutting the plot in z_2 along the direction joining the two pulses and by keeping the temporal dependence, we obtain a spatiotemporal profile, as shown in Fig. 4. It can be seen from Fig. 3 that at z_3 the two large pulses have disappeared whereas from Fig. 4 we see that the pulses have a limited temporal extension.

By taking the half height width of the pulses with $I_c(x, y, z) > 3\bar{I}_c$ and by averaging over more than 100 profiles, we find that the transverse size of a pulse is $250 \pm 50 \mu\text{m}$ whereas its average lifetime is around 0.5 ± 0.1 s. As for the longitudinal extension, by inspecting several movies taken at different z_3 , we estimate it around 30 cm.

The model, derived by coupling the Maxwell equations for the cavity field with a Debye relaxation equation for the refractive index [18], takes into account the Kerr nonline-

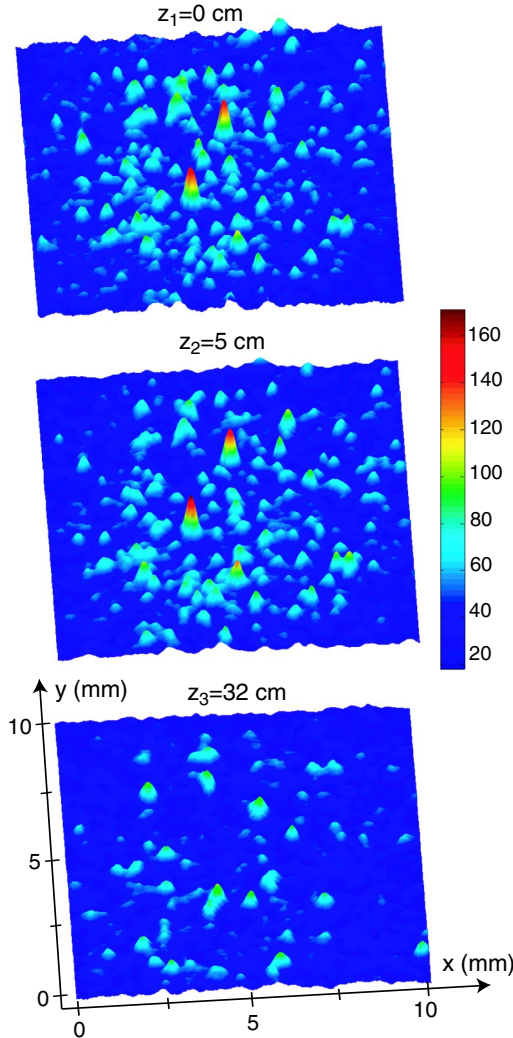


FIG. 3 (color online). Spatial profiles recorded at z_1 , z_2 , and z_3 . Blue (minimal intensity) and red (maximal intensity).

arity of the medium as well as the 2WM mechanism of photon injection inside the cavity. The LCLV is positioned in $z = 0$, perpendicularly to the cavity axis and \vec{r}_\perp denotes the coordinates in the transverse (x, y) plane. The refractive index $n(r_\perp, t)$ satisfies the equation $\tau \partial_t n = n_c - n + l_0^2 \nabla_\perp^2 n - \alpha |E(\vec{r}_\perp, t)|^2$, where ∇_\perp^2 is the transverse Laplacian, l_0 the transverse diffusion length, and $\alpha > 0$ the nonlinear coefficient of the valve, n_c , a constant value determined by the voltage V_0 .

The total electric field at the entrance of the liquid crystal layer is $E(\vec{r}_\perp, t) = E_p e^{i(\vec{k}_p \cdot \vec{r} - \omega_p t)} + E_c e^{i(k_c z - \omega_p t)} + \text{c.c.}$, where $E_c = E_c(\vec{r}_\perp, t)$ is the complex amplitude of the cavity field and E_p is the amplitude of the pump plane wave, which is taken as constant. The intensity, $|E|^2 = |E_p|^2 + |E_c|^2 + (E_p^* E_c / 2) e^{-i\vec{k}_\perp \cdot \vec{r}_\perp} + \text{c.c.}$, gives rise to a refractive index change with two components, one varying slowly in space and the other corresponding to a spatial grating with wave number $\vec{k}_\perp = \vec{k}_p - \vec{k}_c$. We thus write the refractive index as $n = n_c - \alpha |E_p|^2 + n_0 + n_1 e^{-i\vec{k}_\perp \cdot \vec{r}_\perp} + \text{c.c.}$, where $|E_p|^2$ is constant. When we substitute this expression in the equation for n we obtain

$$\begin{aligned} \tau \frac{\partial n_0}{\partial t} &= (-1 + l_0^2 \nabla_\perp^2) n_0 - \alpha |E_c|^2, \\ \tau \frac{\partial n_1}{\partial t} &= (-1 + l_0^2 \nabla_\perp^2 + l_0^2 |\vec{k}_\perp|^2) n_1 - 2i l_0^2 \vec{k}_\perp \cdot \vec{\nabla} n_1 \\ &\quad + -\alpha E_p^* E_c \end{aligned} \quad (1)$$

for the slowly varying fields n_0 and n_1 . The wave equation for the cavity field is written for a planar cavity by adopting the slowly varying amplitude approximation and by considering n_0 and n_1 small. Because of the large scale separation between the medium response time and the cavity round-trip time, we neglect the time derivative and get

$$\begin{aligned} \frac{\partial E_c}{\partial z} &= \left[\frac{i}{2k_c} \nabla_\perp^2 + ik_c n_0 W(z) + \frac{i\delta - \gamma_c}{c} \right] E_c \\ &\quad + ik_c n_1 W(z) E_p(z), \end{aligned} \quad (2)$$

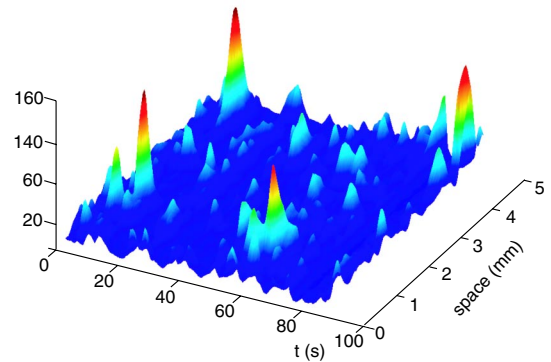


FIG. 4 (color online). Spatiotemporal profile extracted from the z_2 movie.

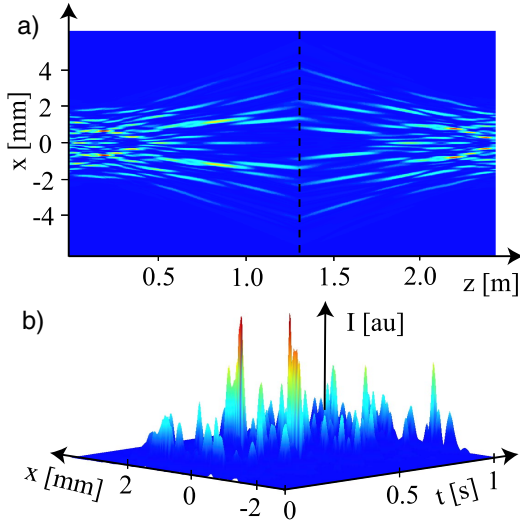


FIG. 5 (color online). Numerically calculated field distributions: (a) a cut in the x - z plane at a fixed time; (b) a spatiotemporal profile at a fixed z . The dashed line marks the lens position ($L_1 = 1.3$ m, $L_2 = 1.1$ m, and $f = 0.7$ m).

where $W(z) = 1$ in the liquid crystal layer and 0 elsewhere, δ is the frequency detuning between the lowest order cavity mode and the pump field, γ_c is the cavity loss rate, and $E_p(0) = E_p$.

Since the liquid crystal layer is thin, inside the medium we neglect the transverse Laplacian and we consider the 2WM in the Raman-Nath diffraction regime [16]. Thus, inside the medium we have to take into account multiple order scatterings of the pump [19]. By doing this, we obtain $E_c(d) = e^{ik_c d n_0} [J_0(2k_c d |n_1|) E_c(0) + iJ_1(2k_c d |n_1|) E_p(0)]$. Outside the LCLV the field evolution is governed by diffraction; thus, the transverse Laplacian has to be retained. By considering that the cavity field has to satisfy the periodic boundary conditions imposed by the cavity, including the presence of the lens [19], it can be shown that the field at the entrance of the LCLV is given by

$$E_c = i \sum_{m=0}^{\infty} \hat{B}^m \hat{C} E_p(0), \quad (3)$$

where the \hat{B} and \hat{C} are operators expressed as

$$\begin{aligned} \hat{B} &= e^{i(L_2/2k_c)\nabla_{\perp}^2} e^{-i(k_c/2f)\tilde{r}_{\perp}^2} e^{i(L_1/2k_c)\nabla_{\perp}^2 + (i\delta - \gamma_c/c)L} \\ &\quad \times e^{idkn_0 J_0(2k_c d |n_1|)}, \\ \hat{C} &= e^{i(L_2/2k_c)\nabla_{\perp}^2} e^{-i(k_c/2f)\tilde{r}_{\perp}^2} e^{i(L_1/2k_c)\nabla_{\perp}^2 + (i\delta - \gamma_c/c)L} \\ &\quad \times e^{idkn_0 J_1(2k_c d |n_1|)}, \end{aligned}$$

with L_1 the distance between the LCLV and the lens, $L_2 = L - L_1$. The first term of the sum, $E_c^{(0)} = i\hat{C}E_p(0)$, accounts for the field generated by the pump in one cavity

round trip. The following terms sum up the field evolutions on the successive cavity loops.

We have performed numerical simulations for one transverse dimension x . The parameters are chosen from the experiment, $\tau = 40$ ms, $l_0 = 30$ μ m, $I_p = 2$ mW/cm², and $\alpha = 4$ cm²/W. The number of terms in the sum is truncated to the number of round trips given by the average lifetime of photons in the cavity. In Fig. 5(a) we show the intensity distribution calculated in the x , z plane at a fixed time, whereas in Fig. 5(b) is shown a spatiotemporal profile at a fixed z . As in the experiment, we observe spatiotemporal pulses confined both in the transverse and z direction.

In conclusion, we have shown a new type of nonlinear optical oscillator, which includes a thin LCLV as the gain medium, and we have given evidence of 3D localized spatiotemporal pulses.

U. B. acknowledges the support of *Ville de Paris*. A. M. acknowledges the support of *Ente Cassa di Risparmio di Firenze*, under the project “dinamiche cerebrali caotiche”.

-
- [1] J.L. Bougrenet de la Tocnaye, P. Pellat-Finet, and J.P. Huignard, *J. Opt. Soc. Am. B* **3**, 315 (1986).
 - [2] F.T. Arecchi, G. Giacomelli, P.L. Ramazza, and S. Residori, *Phys. Rev. Lett.* **65**, 2531 (1990).
 - [3] D.Z. Anderson and R. Saxena, *J. Opt. Soc. Am. B* **4**, 164 (1987).
 - [4] G. D’Alessandro, *Phys. Rev. A* **46**, 2791 (1992).
 - [5] A. Brignon, I. Bongrand, B. Loiseaux, and J.P. Huignard, *Opt. Lett.* **22**, 1855 (1997).
 - [6] U. Bortolozzo, S. Residori, and J.P. Huignard, *Opt. Lett.* **31**, 2166 (2006).
 - [7] Y. Silberberg, *Opt. Lett.* **15**, 1282 (1990).
 - [8] M. Tlidi, and P. Mandel, *Phys. Rev. Lett.* **83**, 4995 (1999).
 - [9] M. Brambilla, L. Columbo, and T. Maggipinto, *J. Opt. B* **6**, S197 (2004).
 - [10] See e.g. P. Coullet, *Chaos* **12**, 2445 (2002).
 - [11] N. Akhmediev, J.M. Soto-Crespo, and G. Town, *Phys. Rev. E* **63**, 056602 (2001).
 - [12] O. Cohen, G. Bartal, H. Buljan, T. Carmon, J.W. Fleischer, and M. Segev, *Nature (London)* **433**, 500 (2005).
 - [13] S. Dyachenko, A.C. Newell, A. Pushkarev, and V.E. Zakharov, *Physica (Amsterdam)* **57D**, 96 (1992).
 - [14] S.A. Ponomarenko and G.P. Agrawal, *Opt. Commun.* **261**, 1 (2006).
 - [15] P. Gunter and J.P. Huignard, *Photorefractive Crystals and Their Applications* (Springer-Verlag, Berlin, 1989).
 - [16] A. Yariv, *Optical Waves in Crystals* (Wiley, New York, 2003).
 - [17] U. Bortolozzo, P. Villoresi, and P.L. Ramazza, *Phys. Rev. Lett.* **87**, 274102 (2001).
 - [18] A.C. Newell and J. Moloney, *Nonlinear Optics* (Addison-Wesley, Reading, MA, 1991).
 - [19] The full derivation of the model will be reported elsewhere (article in preparation).